ELSEVIER

Journal of Power Sources 104 (2002) 132–139

JOURNAL OF POWER SOURCES

www.elsevier.com/locate/jpowsour

Suppressive effect of Li_2CO_3 on initial irreversibility at carbon anode in Li-ion batteries

Yong-Kook Choi[a,*], Kwang-il Chung[a], Woo-Seong Kim[b], Yung-Eun Sung[b], Su-Moon Park[c]

[a]*Department of Chemistry and RRC/HECS, Chonnam National University, Kwangju 500-757, South Korea*
[b]*Department of Materials Science and Engineering, K-JIST, Kwangju 500-712, South Korea*
[c]*Department of Chemistry and Center for Integrated Molecular Systems, Pohang University of Science and Technology, Pohang 790-784, South Korea*

Received 4 June 2001; accepted 20 August 2001

Abstract

The initial capacity irreversibility caused by film formation on a mesophase pitch-based carbon fibre (MPCF) electrode surface is studied with the goal of improving the performance of a lithium-ion battery. The addition of Li_2CO_3 to a solution of 1 M $LiPF_6$/EC:DFC (1:1, v/v) results in a decrease in the initial irreversible capacity caused by solvent decomposition and the passivation film on the MPCF electrode surface. Suppression of the initial irreversible capacity at the anode electrode by the introduction of Li_2CO_3 is investigated by means of chronopotentiometry, cyclic voltammetry, ac impedance spectroscopy, FTIR, scanning electron microscopy (SEM), and energy dispersive X-ray (EDX) analysis. It is concluded that the suppression is caused mainly by prevention of solvent decomposition and by structural change in the passivation film on the anode electrode.

Keywords: Lithium-ion battery; Initial irreversible capacity; Additive; Carbon anode

1. Introduction

Lithium-ion batteries are generally composed of a lithium-containing transition metal oxide as the cathode electrode material and a carbon material as the anode electrode [1–4]. When initially intercalated into the carbon anode, a portion of the lithium is lost from the electrode as a result of irreversible side-reactions. Typically, these reactions involve: (i) solvent decomposition at the carbon electrode surface; (ii) irreversible reaction of lithium-ions with functional groups such as carboxyl, hydroxyl and carbon hydride on the carbon surface; (iii) the irreversible insertion of lithium into carbon. In particular, (i) and (ii) lead to the formation of a passivation film or solid electrolyte interface (SEI) on the carbon electrode surface [5–11]. Many researchers have studied the formation mechanism of the pasivation film on the carbon electrode. Overall, the irreversibility reduces the capacity of the electrode from its theoretical value [12].

A number of researchers have examined possible routes for removing the initial irreversible capacity [13,14]. It has been shown that the passivation film is formed via reactions between carbon and electrolyte. The resulting film blocks further electrolyte reduction while allowing continued lithium-ion insertion so that the side-reactions are suppressed after the first cycle [15,16]. The formation of the passivation film on carbon surface causes a decrease in the capacity of the cathode ($LiCoO_2$, $LiMn_2O_4$, $LiNiO_2$) and as a result, new routes to the formation of a passivation film on the carbon surface without solvent decomposition and the irreversible reaction of the lithium-ions with functional groups on the carbon surface is highly desirable.

The growth and properties of the SEI depend on the electrolyte composition, the nature of impurities, and the additives employed. For example, the addition of SO_2 [17], CO_2 [18–20], or inorganic agents such as Ni and Sn [21,22] has been shown to promote deposition of passivation films, and thus, prevent the reduction of the majority of the components of the electrolyte. This paper describes the use, for the first time, of Li_2CO_3 as the additive for the formation of a passivation film on the carbon surface to suppress the initial irreversible capacity. Chronopotentiometry, cyclic voltammetry, and impedance spectroscopy are used to investigate the effects of the Li_2CO_3 additive. Scanning electron microscopy (SEM), energy dispersive X-ray (EDX) analysis and FTIR are

* Corresponding author. Fax: +82-62-530-3389.
E-mail address: ykchoi@chonnam.ac.kr (Y.-K. Choi).

0378-7753/02/$ – see front matter
PII: S0378-7753(01)00911-9

also used to monitor changes in the surface morphology and composition due to the formation of the passivation film caused by solvent decomposition and the precipitation of Li_2CO_3.

2. Experimental

The mesophase pitch-based carbon fibre (MPCF) electrode was prepared by mixing MPCF powder (Petoca Co. Ltd.) with polyvinyldifluoride (PVDF) as a binder, followed by pressing on to a copper foil. After vacuum drying at 120 °C for 6 h, the electrode was placed in a three-electrode cell under an argon atmosphere. Lithium metal was used as both the counter and the reference electrodes. The reference electrode was sandwiched between a square MPCF electrode (1 cm^2) and a Li counter electrode, and was separated with a Celgard polypropylene separator. This fabrication was performed under an atmosphere of argon. The cycling tests of an MPCF electrode were conducting with a WBCS3000 battery cycler system (Won-A Tech). The electrochemical properties of the passivation film on the MPCF were investigated using an organic electrolyte system. High-purity ethylene carbonate (EC, 99.99%) and 1,2-diethyl carbonate (DEC, >99.99%) (Mitsubishi Chemical, battery grade) were used as solvents for the electrolyte solution. Lithium hexafluoro phosphate, $LiPF_6$ (Morita Chemical Industry), was used as the electrolytic salt. Lithium carbonate, Li_2CO_3 (Aldrich), was added to the prepared electrolyte. In fact, Li_2CO_3 dissolves with difficulty in the organic solvent and it was therefore, necessary to stir the solution for a week in order to obtain a solution.

Finally, however, an electrolyte that was saturated with Li_2CO_3 was obtained. The concentrations of Li_2CO_3 additive were determined using the relationship between absorbance and concentration. A calibration curve was prepared from a series of standard solutions of Li_2CO_3, viz. 0.1, 0.3, 0.5, 1.0, 2.0, and 3.0 mM. The absorbance of solution was measured using UV spectroscopy (Hewlett Packard 8425A). The concentration of saturated Li_2CO_3 was 7 mM from the absorbance measurement.

Chronopotentiometry and cyclic voltammetry were used to study the initial irreversible capacities and the voltage of solvent decomposition. The properties of the passivation film on the MPCF and the first intercalation of Li^+ in MPCF through the passivation film were investigated by ac impedance spectroscopy by means of a Potentiostat/Galvanostat (EG&G model 273A) and Lock-in Amplifier (EG&G model 5210). An impedance measurement was performed by applying the previously measured open-circuit potential, overlaid with a 5 mV harmonic perturbation signal in the frequency range from 100 kHz to 10 mHz. These measurements were carried out at room temperature.

SEM/EDX analyses were undertaken on the samples using a JSM-5400 Scanning Microscope (NORAN Instruments). The working voltage was set at 20 kV and the working distance of the lens at 27 md. After the MPCF electrode was intercalated to 0.0 V (versus Li/Li^+) and de-intercalated to 2.0 V (versus Li/Li^+), the sample was rinsed with DEC to remove the electrolyte and dried in vacuum.

A Nicolet FTIR spectrometer functioning in the range 4000–700 cm^{-1} was used to determine the chemical composition of the passivation film. The de-intercalated MPCF was directly examined by a Nicolet FTIR spectrometer that was continuously purged with nitrogen gas to minimise water vapour and atmospheric CO_2.

3. Results and discussion

The typical voltage–capacity profile of an MPCF electrode at a low rate of 0.5 mA cm^{-2} in 1 M $LiPF_6$/EC:DEC (1:1, v/v) without the additive, Li_2CO_3 is shown in Fig. 1(a). The initial irreversible capacity was about 80 mAh g^{-1}, which was calculated by subtracting the initial de-intercalation capacity from the initial intercalation capacity. The voltage capacity profile of an MPCF electrode in 1 M $LiPF_6$/EC:DEC (1:1) containing Li_2CO_3 additive is given in Fig. 2(a). The initial irreversible capacity is decreased to about 50 mAh g^{-1}. Thus, the irreversible capacity is reduced by 38%. In addition, Figs. 1(b) and 2(b) show plots of $-dQ/dV$ versus V for MPCF electrodes to understand the difference in the initial intercalation/de-intercalation behaviour of the carbon without and with Li_2CO_3. The initial intercalation peaks are at 0.04 and 0.03 V (versus Li/Li^+) and the de-intercalation peaks at 0.11 and 0.14 V (versus Li/Li^+) in the electrolyte without Li_2CO_3 (Fig. 1(b)). In the electrolyte with Li_2CO_3 (Fig. 2(b)), however, the initial intercalation peaks are at 0.05 and 0.04 V (versus Li/Li^+) and the de-intercalation peaks at 0.10 and 0.13 V. In the electrolyte with Li_2CO_3, the initial intercalation peaks are shifted positively and the initial de-intercalation peaks were shifted negatively. In other words, the intercalation/de-intercalation of the MPCF electrode in the electrolyte with Li_2CO_3 is easier than that in the electrolyte without Li_2CO_3. These results explain that the properties of the passivation film on the MPCF electrode surface are improved in the electrolyte with Li_2CO_3.

A portion of the initial irreversible capacity is caused by solvent decomposition on the MPCF electrode surface. The irreversible reaction of lithium-ions with functional groups of carbon surface and the irreversible insertion of the lithium into the MPCF electrode also play a role. In Figs. 1(a) and 2(a), the main differences without and with Li_2CO_3 are the profile at the voltage range from the open-circuit voltage (3.1 V) to 0.5 V (versus Li/Li^+), as is obvious from the first intercalation curve. As a result, attention is placed on the irreversible capacity caused by solvent decomposition in these voltage regions. The irreversible capacity is about 20 mAh g^{-1} in this region (Fig. 1). The origin of these regions is investigated by means cyclic voltammetry.

Cyclic voltammograms for an MPCF electrode in 1 M $LiPF_6$/EC:DEC (1:1) are presented in Fig. 3. The scan rate is

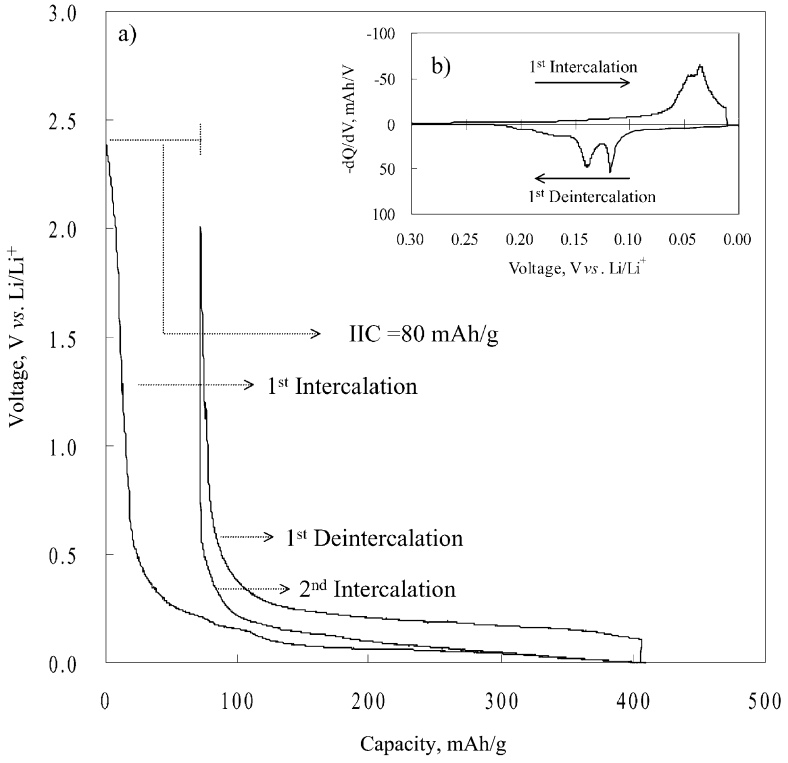

Fig. 1. (a) Voltage–capacity profile and (b) plot of $-dQ/dV$ vs. V of MPCF electrode in 1 M $LiPF_6$/EC:DEC (1:1). Current density is 0.5 mA cm^{-2}.

1 mV s^{-1} and voltage range is 3–0 V (versus Li/Li^+). The solvent decomposition is identified as irreversible cathodic peaks at about 2.2, 2.0, and 0.7 V in the initial intercalation process. The reduction of solvent was irreversible. As can be seen, the decomposition of DEC and EC occurred at different potentials. In our previous work [23], the cyclic voltammograms were measured in pure DEC and pure EC dissolved with $LiPF_6$ to define the decomposition potentials

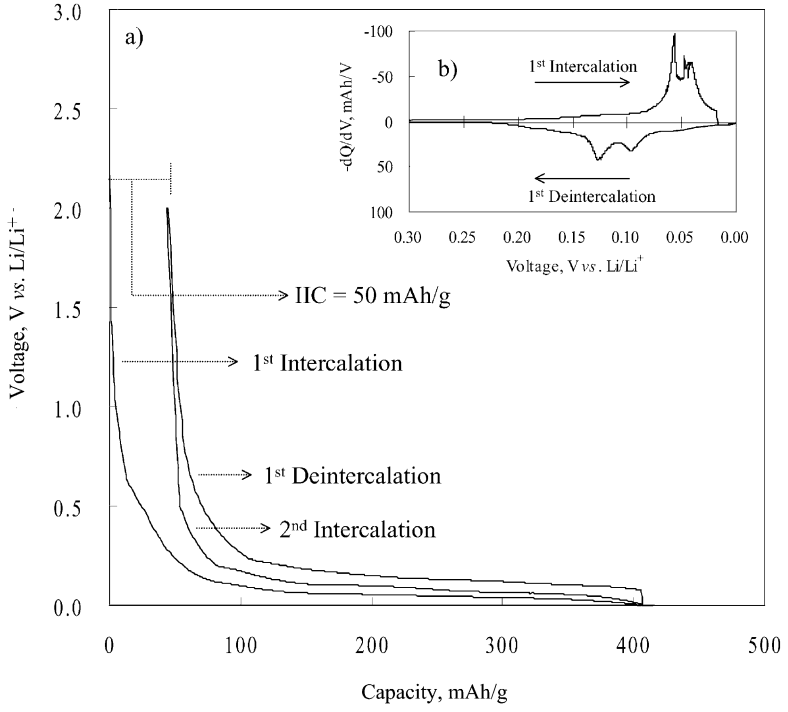

Fig. 2. (a) Voltage–capacity profile and (b) plot of $-dQ/dV$ vs. V of an MPCF electrode in 1 M $LiPF_6$/EC:DEC (1:1) with added Li_2CO_3. Current density is 0.5 mA cm^{-2}.

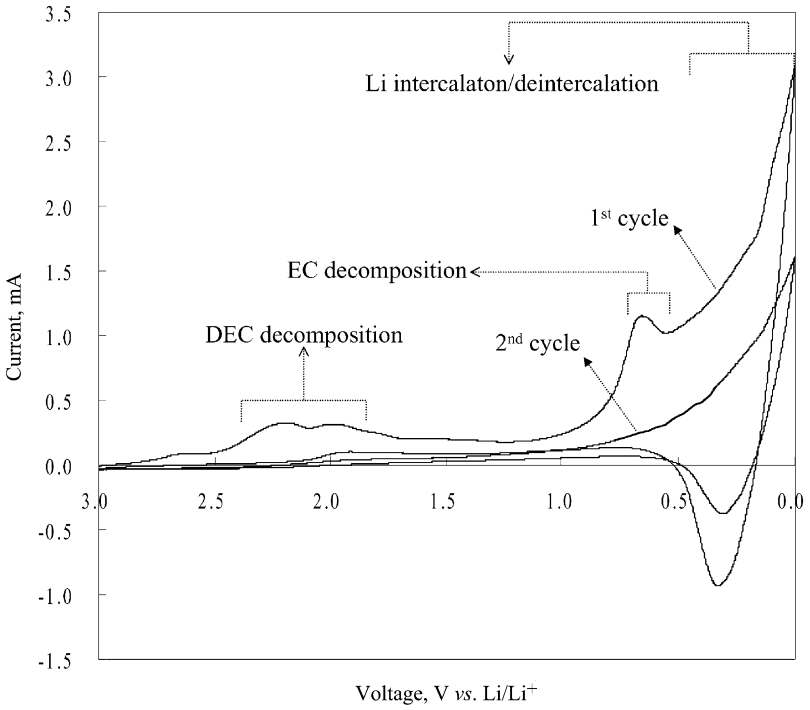

Fig. 3. Cyclic voltammograms of MPCF electrode in 1 M $LiPF_6$/EC:DEC (1:1). Scan rate is 1 mV s^{-1}.

of DEC and EC. According to the results, the decomposition of pure DEC occurred at 2.2 and 2.0 V (versus Li/Li^+) and the decomposition of pure EC occurred at 0.7 V (versus Li/Li^+). It is reasonable that the decomposition of DEC occurs at higher potential than that of EC since DEC, a linear carbonate solvent, is less stable than a cyclic carbonate such as EC. In addition, the peak that appears at about 2.7 V may be due to the irreversible reaction of lithium-ions with functional groups on the carbon surface, or the effect of traces of water. No peaks for the solvent decomposition appeared in a second scan. This suggests that the passivation film blocks, the further reduction of solvent while allowing continued lithium-ion

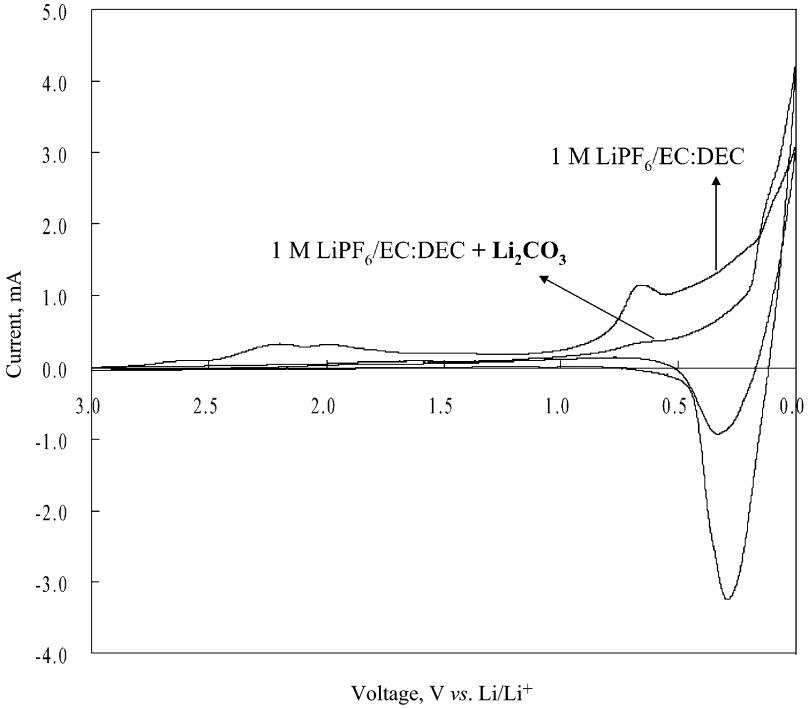

Fig. 4. Cyclic voltammograms of MPCF electrode in 1 M $LiPF_6$/EC:DEC (1:1) and in 1 M $LiPF_6$/EC:DEC (1:1) with added Li_2CO_3. Scan rate is 1 mV s^{-1}.

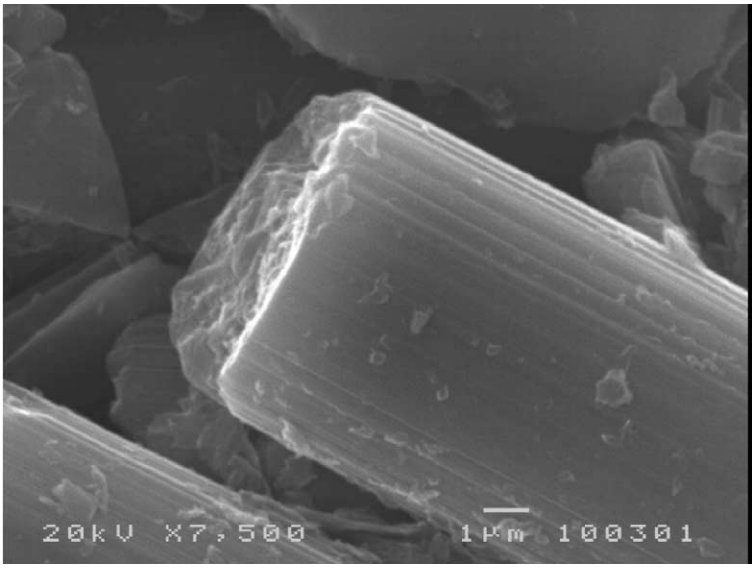

Fig. 5. SEM image of original MPCF electrode surface.

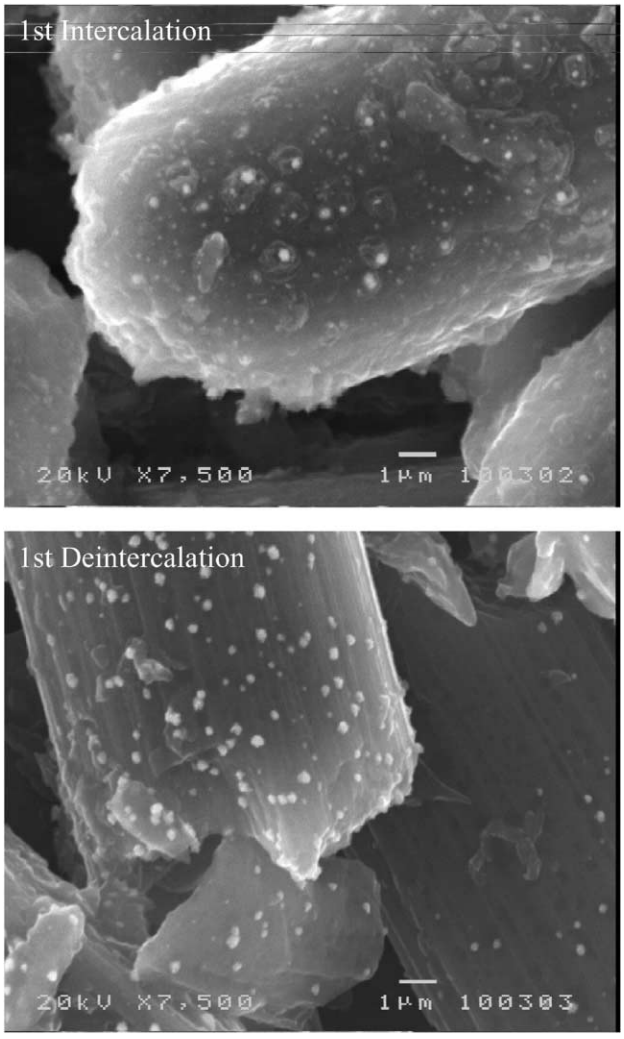

Fig. 6. SEM images of MPCF electrode surface after intercalation/deintercalation in 1 M $LiPF_6$/EC:DEC (1:1).

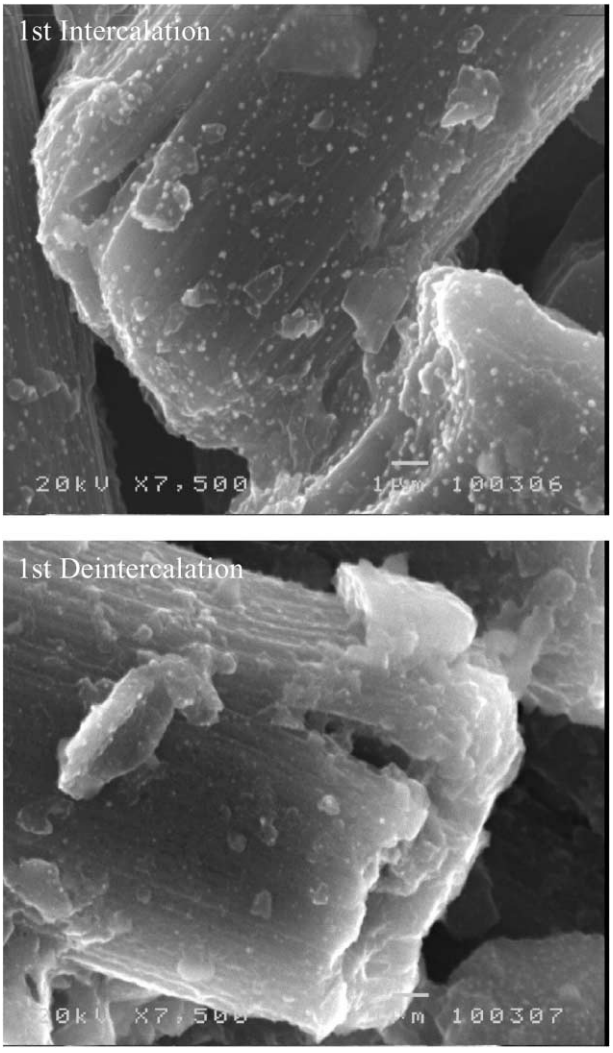

Fig. 7. SEM images of MPCF electrode surface after intercalation/deintercalation in 1 M $LiPF_6$/EC:DEC (1:1) with added Li_2CO_3.

insertion so that side-reactions are suppressed after the initial intercalation. Therefore, no further decomposition occurs on the second cycle, since the passivation film is already formed on the MPCF electrode surface, as a result of the initial intercalation. This provides clear evidence that the irreversible capacity is due to solvent decomposition and is consistent with previous results [13,14].

The suppression of solvent decomposition by added Li_2CO_3 can be clearly seen from cyclic voltammograms, as shown in Fig. 4. This gives a comparison of the cyclic voltammograms of the first scan of the MPCF electrode in 1 M $LiPF_6$/EC:DEC (1:1) and 1 M $LiPF_6$/EC:DEC (1:1) containing 7 mM Li_2CO_3. In the case of added Li_2CO_3, reduction peaks caused by EC and DEC decomposition virtually disappear. This is the clearest evidence that solvent decomposition was suppressed by Li_2CO_3 additive. It would appear that the saturated Li_2CO_3 in the electrolyte is deposited on the MPCF electrode surface before reaching the voltage for solvent decomposition. Therefore, the passivation film formed in the presence of Li_2CO_3 prevents solvent decomposition and co-intercalation, and also permits the intercalation of Li^+ into the MPCF electrode.

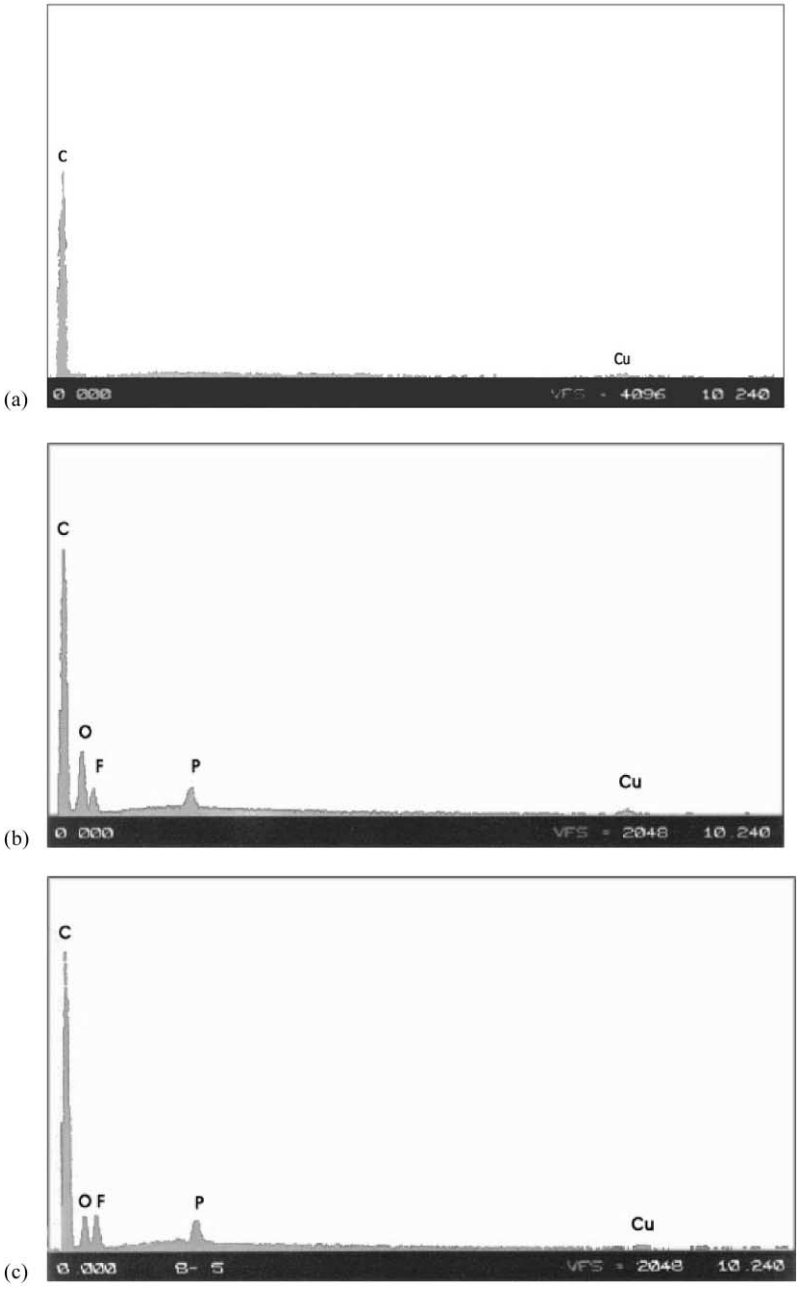

Fig. 8. EDX data of (a) original MPCF electrode, (b) after intercalation in 1 M $LiPF_6$/EC:DEC (1:1), (c) after intercalation in 1 M $LiPF_6$/EC:DEC (1:1) + Li_2CO_3.

To confirm the above results, the surface morphologies of the MPCF electrode have been observed by SEM. The original MPCF electrode surface was first measured, in order to provide a comparison with the initial intercalated electrode surface. The original MPCF electrode surface, on which carbon fibres are distributed, is shown in Fig. 5. The average diameter of the MPCF is about 8 μm, but the length is not regular. Fig. 6 shows the electrode surface after Li^+ intercalation into the MPCF electrode with 0.5 mA cm^{-2} in the 1 M $LiPF_6$/EC:DEC (1:1) electrolyte without a Li_2CO_3 additive. The surface of the intercalated MPCF electrode has a clearly different surface morphology from the original surface. The electrode intercalated to 0.0 V (versus Li/Li^+) and de-intercalated to 2.0 V is covered with fine deposits. Based on existing papers [24–27], the deposit consists of $ROCO_2Li$, Li_2CO_3, ROLi, LiOH, LiF, which represent the products of solvent decomposition. In this case, it could be assumed that the passivation film formed by decomposition of EC and DEC covered the surfaces of the carbon fibres. The surface of the MPCF electrode that has been intercalated and de-intercalated in the electrolyte in the presence of the Li_2CO_3 additive is shown in Fig. 7. This micrograph shows the fine deposits that are formed on the MPCF electrode surface which are less dense than those in Fig. 6. Also the carbon fibres are well distributed as in the original MPCF surface (Fig. 5). The solvent decomposition of EC and DEC is strongly suppressed by the added Li_2CO_3 as is seen in the cyclic voltammogram given in Fig. 4.

EDX data are given in Fig. 8 for the original MPCF electrode and the MPCF electrodes after a period of charging in the electrolyte with and without Li_2CO_3. The EDX data of the original MPCF electrode (Fig. 8(a)) shows only the peaks of C and Cu. The C peak is due to the carbon electrode and the Cu peak to the Cu current-collector. Peaks for O, P, and F were not detected for the original MPCF electrode. Therefore, the O, P, and F peaks in Fig. 8(b) and (c) are due to the passivation film on carbon electrode surface. Generally, the products of the solvent decomposition are known to be $ROCO_2Li$, Li_2CO_3, ROLi, LiOH, Li_2O, LiF [24–27]. The EDX results (Fig. 8(b) and (c)) show peaks corresponding to O, F and P with and without Li_2CO_3 additive. The P and F peaks are likely to be due to PF_6^- ions, which have been inserted in the passivation film in both cases. On the other hand, the O peak is clearly reduced in the presence of the Li_2CO_3 additive, which explains the reduced level of solvent decomposition. This is consistent with the cyclic voltammetric data in Fig. 4.

To obtain additional information on the chemical composition of the first intercalated MPCF surface in the electrolyte without and with Li_2CO_3, FTIR-ATR is used. The FTIR-ATR spectra obtained from the MPCF surface are presented in Fig. 9. The spectrum of the original electrode shows no absorption bands (Fig. 9(a)). The FTIR-ATR spectrum for the intercalated MPCF surface in the electrolyte without the additive is given in Fig. 9(b). A number of absorption bands can be seen. These absorption bands,

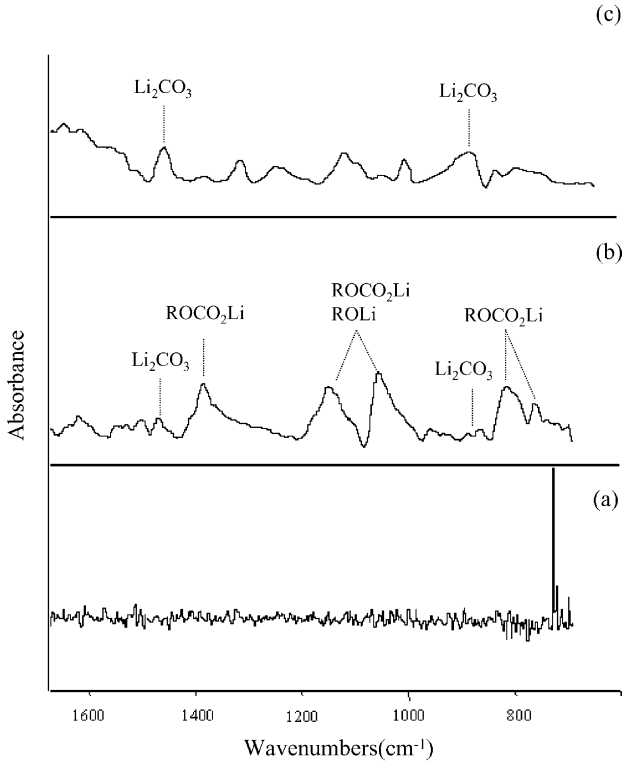

Fig. 9. FTIR spectra of (a) original MPCF electrode surface, (b) after intercalation in 1 M $LiPF_6$/EC:DEC (1:1), (c) after intercalation in 1 M $LiPF_6$/EC:DEC (1:1) + Li_2CO_3.

which are produced during the first cycle, are related to the film caused by the electrolyte decomposition. According to the literature [24,26,28], the bands at 1437 and 867 cm^{-1} are due to Li_2CO_3. The bands at 1390 (C=O, s), 1070–1150 (C–O, as), and 840–820 cm^{-1} ($–CO_3^{2-}$) correspond to $ROCO_2Li$ and ROLi. In the presence of Li_2CO_3 (Fig. 9(c)), the main peaks for $ROCO_2Li$ and ROLi have nearly disappeared. These findings suggest that the addition of Li_2CO_3 suppresses solvent decomposition. This result is also consistent with the cyclic voltammetric and EDX data.

Impedance spectroscopy is used to compare the resistance of the passivation films formed by the decomposition of EC and DEC and precipitation of Li_2CO_3. The impedance spectra of the MPCF electrode after first intercalation in the two different electrolytes are given in Fig. 10. The diagrams show two semicircles on a complex plane. The two semicircles are clearer for the electrolyte which contains Li_2CO_3. Semicircles in a high-frequency region correspond to the passivation film and those in a low-frequency are derived from the charge transfer between the electrolyte and the electrode interface [29]. To investigate differences in the passivation film between the electrolyte with and without Li_2CO_3, the film resistance was measured in the high-frequency range of 100 kHz to 10 Hz, by means of a non-linear, least-squares fitting procedure. The film resistance decreases from 26 to 5 Ω in the electrolyte that contains Li_2CO_3. The passivation film in the electrolyte

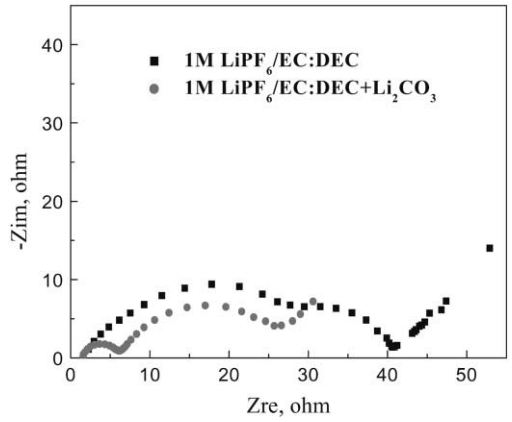

Fig. 10. Impedance spectra of MPCF electrode after intercalation (a) in 1 M $LiPF_6$/EC:DEC (1:1) and (b) in 1 M $LiPF_6$/EC:DEC (1:1) + Li_2CO_3.

with the additive is formed mainly by the precipitation of Li_2CO_3. By contrast, films produced by the decomposition of EC and DEC contain many components such as Li_2CO_3, $RLiCO_3$, LiOH, Li_2O and LiF. Therefore, it is entirely possible that the film formed by precipitation of Li_2CO_3 has a higher conductivity than the film formed by decomposition of EC and DEC.

Finally, XRD analysis of the carbon has been conducted before and after cycling with and without the Li_2CO_3 additive. From the results, the (0 0 2) peaks are shifted after charge, but are not changed with and without the additive. Therefore, the additive does not affect the carbon anode.

4. Conclusions

The study presents the first observation that the initial irreversible capacity of the MIPCF electrode can be decreased by the addition of Li_2CO_3 into 1 M $LiPF_6$/EC:DEC (1:1, v/v) electrolyte. The decrease in irreversible capacity is caused by suppression of solvent decomposition, which is confirmed by cyclic voltammetry, SEM, EDX, FTIR and ac impedance spectroscopy. The passivation film formed by the precipitation of Li_2CO_3 inhibits solvent decomposition and has a relatively lower resistance. Therefore, compared with no additive electrolyte, the addition of Li_2CO_3 to the electrolyte has two advantages, viz. it forms a passivation film with a low resistance on MPCF electrode surface and suppresses the decomposition of EC and DEC. The might provide practical process for reducing the initial irreversibility and is promising in terms of improving the performance of a lithium-ion battery. Further studies are required to reveal the chemical mechanism of the suppression of the solvent decomposition and the role of the predeposited Li_2CO_3 film.

Acknowledgements

This work was supported by the Center for Integrated Molecular Systems of Postech, under KOSEF.WSK and YES acknowledge the financial support from the BK 21 Project of the Ministry of Education.

References

[1] J.O. Besenhard, Handbook of Battery Materials, Wiley, New York, 1999, p. 383.
[2] N. Imanishi, S. Ohashi, T. Ichikawa, T. Takeda, O. Yamamoto, J. Power Sources 26 (1992) 535.
[3] Y. Mohri, T. Iriyama, T. Hashimoto, S. Yamazaki, F. Fawakami, H. Shiroki, T. Yamabe, J. Power Sources 56 (1995) 205.
[4] H. Fujimoto, A. Mabuchi, K. Tokumitsu, T. Kasuh, J. Power Sources 54 (1995) 440.
[5] R. Fong, U.V. Sacken, J.R. Dahn, J. Electrochem. Soc. 137 (1990) 2009.
[6] E. Peled, C. Menachem, D. Bar-Tow, A. Melman, J. Electrochem. Soc. 143 (1996) L4.
[7] K. Suzuki, T. Hamada, T. Sugiura, J. Electrochem. Soc. 146 (1999) 890.
[8] C. Chung, S. Jun, K. Lee, M. Kim, J. Electrochem. Soc. 146 (1999) 1664.
[9] R. Yazami, Electrochim. Acta 45 (1999) 87.
[10] M. Inaba, Y. Kawatate, A. Funabiki, S. Jeong, T. Abe, Z. Ogumi, Electrochim. Acta 45 (1999) 99.
[11] Y.-K. Choi, J.-G. Park, K.-i. Chung, S.-K. Kim, W.-S. Kim, Microchem. J. 64 (2000) 227.
[12] P. Arora, R.E. White, J. Electrochem. Soc. 145 (1998) 3647.
[13] K. Kanamura, H. Tamura, S. Shiraishi, Z. Takehara, J. Electroanal. Chem. 394 (1995) 49.
[14] Z.X. Shu, R.S. Mcmillan, J.J. Murray, J. Electrochem. Soc. 140 (1993) 922.
[15] Y. Ein-Eli, S.F. McDevitt, J. Electrochem. Soc. 142 (1995) 1746.
[16] M.C. Snart, B.V. Ratnakumar, S. Surampudi, Y. Wang, X. Zhang, S.G. Greenbaum, A. Hightower, C.C. Ahn, B. Fultz, J. Electrochem. Soc. 146 (1999) 3963.
[17] Y. Ein-Eli, S.R. Thomas, V.R. Koch, J. Electrochem. Soc. 144 (1997) 1159.
[18] T. Osaka, T. Momma, Y. Matsumoto, Y. Uchida, J. Electrochem. Soc. 144 (1997) 1709.
[19] T. Osaka, T. Momma, T. Tajima, Y. Matsumeto, J. Electrochem. Soc. 142 (1995) 1057.
[20] M. Winter, R. Imhof, F. Joho, P. Novak, J. Power Sources 81 (1999) 818.
[21] O. Mao, R.A. Dunlap, J.R. Dahn, J. Electrochem. Soc. 146 (1999) 405.
[22] P. Yu, J.A. Ritter, R.F. White, B.N. Popov, J. Electrochem. Soc. 147 (2000) 1280.
[23] Y.-K. Choi, K.-i. Chung, W.-S. Kim, Y.-E. Sung, Microchem. J. 68 (2001) 61.
[24] D. Aurbach, A. Zaban, Y. Gofer, Y.E. Ely, I. Weissman, O. Chusid, O. Abaramson, J. Power Sources 54 (1995) 76.
[25] D. Aurbach, Y. Ein-Eli, O. Chusid, J. Electrochem. Soc. 141 (1994) 603.
[26] D. Aurbach, Y. Ein-Eli, B. Markovsky, A. Zaban, J. Electrochem. Soc. 142 (1995) 2882.
[27] Y. Matsumura, S. Wang, J. Mondori, J. Electrochem. Soc. 142 (1995) 2914.
[28] D. Aurbach, Y. Ein-Eli, O. Chusid, J. Electrochem. Soc. 141 (1994) 603.
[29] K.-I. Chung, B.-D. Choi, S.-K. Kim, W.-S. Kim, Y.-K. Choi, J. Korean Electrochem. Soc. 1 (1998) 28.